# Constraints on the Lee-Wick Higgs Sector

Christopher D. Carone  $^{1,\,*}$  and Reinard Primulando  $^{1,\,\dagger}$ 

<sup>1</sup>Department of Physics, College of William & Mary, Williamsburg, VA 23187-8795 (Dated: August, 2009)

### Abstract

Lee-Wick partners to the Standard Model Higgs doublet may appear at a mass scale that is significantly lower than that of the remaining Lee-Wick partner states. The relevant effective theory is a two-Higgs doublet model in which one doublet has wrong-sign kinetic and mass terms. We determine bounds on this effective theory, including those from neutral B-meson mixing,  $b \to X_s \gamma$ , and  $Z \to b\bar{b}$ . The results differ from those of conventional two-Higgs doublet models and lead to meaningful constraints on the Lee-Wick Higgs sector.

<sup>\*</sup>cdcaro@wm.edu

<sup>†</sup>rprimulando@wm.edu

### I. INTRODUCTION

The Lee-Wick Standard Model (LWSM) presents a novel solution for addressing the hierarchy problem in the Standard Model [1]. For every Standard Model field, a gauge-invariant, higher-derivative (HD) kinetic term is introduced so that propagators fall off more quickly with momentum. Although such terms include higher-derivative interactions as well, a power-counting exercise shows that the resulting theory is no more than logarithmically divergent [1]. The dependence of the Higgs boson mass squared on any ultraviolet physics is no worse in the LWSM than it is, for example, in the Minimal Supersymmetric Standard Model (MSSM).

The presence of HD quadratic terms leads to the presence of additional poles in the two-point function of each field. Using an auxilliary field method (that we review in the next section), it is possible to recast the original LWSM Lagrangian in terms of one without HD terms, but with additional fields that correspond to the LW partner states [1]. In this formulation, all interactions in the Lagrangian have mass dimension no greater than four. We refer to this as the LW form of the theory. The enhanced convergence of the LWSM in the HD form is reproduced in the LW form via cancellations between Feynman diagrams involving Standard Model particles and those involving their LW partners. Such diagramatic cancellations are reminiscent of the situation in the MSSM, but differ in a fundamental way: LW particles have the same spin as their Standard Model partners. The cancellation of quadratic divergences is a consequence of the signs of the LW kinetic and mass terms, which are opposite to those of ordinary particles.

It is natural to question the consistency of a theory that includes physical states with "wrong-sign" kinetic and mass terms. These states have negative norms, so that the free Hamiltonian is bounded from below. The presence of eigenstates of the Hamiltonian with real eigenvalues and negative norms, however, can lead to a violation of unitarity. Lee and Wick [2, 3] showed long ago that unitary can be preserved in such a theory if the negative norm states have non-vanishing decay widths, and hence are eigenstates of the Hamiltonian with complex eigenvalues. The S matrix constructed out of the eigenstates of the Hamiltonian with real eigenvalues excludes these states and is unitary. Lee and Wick [2, 3], as well as Cutkosky  $et\ al.\ [4]$  showed how the pole prescription in perturbation theory is modified so that the correct S matrix is produced, and no violation of unitarity was found in

any explicit higher-order calculation that the authors considered. While this construction of the S matrix leads to a violation of causality at a microscopic level, no logical paradoxes have been shown to arise at macroscopic scales [2, 3, 5, 6]. More recently, unitarity of longitudinal gauge boson scattering amplitudes in the LWSM has been demonstrated [7], a result that is not obvious given that LW vector bosons masses do not arise via spontaneous symmetry breaking. In summary, every explicit calculation in LW theories, including nonperturbative studies [8], has supported the consistency of these theories. This motivates phenomenological studies [9, 10, 11, 12, 13, 14, 15, 16, 17] of the LWSM as a viable solution to the hierarchy problem.

Recent work on the LWSM has included studies of collider signals [9], flavor-changing [10] and electroweak precision constraints [11, 12], higher-derivative generalizations [13], running of couplings and unification [14, 15], and LW theories at high-temperature [16]. If the LW particles are assumed to have a common mass,  $M_{LW}$ , then electroweak constraints typically require this scale to be above  $\sim 5$  TeV. However, as pointed out in Ref. [12], the spectrum of LW particles need not be degenerate. The LW partners to the Higgs boson, the top quark, the left-handed bottom quark and the SU(2) gauge bosons give the greatest contributions to the cancellation of the Higgs boson quadratic divergence and must be present at or below the TeV scale. The remaining LW partners could appear around 10 TeV without requiring substantial fine tuning in the Higgs bare mass. The electroweak constraints on the effective theory with this minimal LW particle content was studied in Ref. [12], where it was noted that the LW-mass scale for the Higgs sector  $m_{\tilde{h}}$  was only weakly constrained. While the LW gauge and fermion partners were again forced into the multi-TeV range,  $m_{\tilde{h}}$  could be O(100) GeV without running afoul of the bounds. This result suggests another possible hierarchy in the LW particle spectrum: the LW partners to the Standard Model Higgs doublet could be well below 1 TeV, while the remaining LW states could be substantially heavier than the LW Higgs.

What is interesting about this effective theory is that it is similar to the often-studied two-Higgs doublet (2HD) extensions of the Standard Model. However, the sign difference in the LW kinetic and mass terms leads to sign changes in the LW Higgs propagator as well as in the interaction vertices that originate in the kinetic terms by gauge invariance. Sign differences in specific Feynman diagrams change the theoretical predictions for a number of one-loop processes, so that the resulting bounds on the scale  $m_{\tilde{h}}$  cannot be simply inferred

from the 2HD results; a numerical reanalysis is required. The purpose of this paper is to begin this task, by considering the bounds from neutral B-meson mixing (for both the  $B_d$  and  $B_s$  mesons), the decay  $b \to X_s \gamma$  and the decay  $Z \to b\overline{b}$ . The bounds on the LW Higgs sector substantially supercede those that appear in Ref. [12] and are relevant in determining the parameter space that might be explored in future collider experiments.

Our paper is organized as follows: In Section II, we review the construction of the LW Higgs sector and establish our conventions. In Section III we determine the bounds on the charged LW Higgs from B-meson mixing,  $b \to X_s \gamma$  and  $Z \to b\overline{b}$ . In Section IV we consider the constraints that are implied by these results on the neutral LW Higgs states, and in the final section we summarize our conclusions.

#### II. HIGGS SECTOR OF THE LWSM

The Higgs sector of the LWSM is given by the Lagrangian

$$\mathcal{L}_{HD} = (D_{\mu}\hat{H})^{\dagger}(D^{\mu}\hat{H}) - \frac{1}{m_{\tilde{h}}^{2}}(D_{\mu}D^{\mu}\hat{H})^{\dagger}(D_{\nu}D^{\nu}\hat{H}) - V(\hat{H}), \tag{2.1}$$

where the hat indicates that the field is defined in the HD theory. Since the LW gauge bosons are decoupled from the effective theory of interest, the covariant derivative is given by

$$D_{\mu} = \partial_{\mu} + ig_2 W_{\mu}^a T^a + ig_1 B_{\mu} Y. \tag{2.2}$$

where  $W^a_{\mu}$  and  $B_{\mu}$  are the ordinary  $SU(2)_W$  and  $U(1)_Y$  gauge fields, respectively. Note that the generators are normalized such that Tr  $T^aT^b=1/2$  and  $Y\hat{H}=1/2\hat{H}$ . The potential  $V(\hat{H})$  takes the form

$$V(\hat{H}) = \frac{\lambda}{4} \left( \hat{H}^{\dagger} \hat{H} - \frac{v^2}{2} \right)^2. \tag{2.3}$$

In order to eliminate the higher-derivative term in Eq. (2.1), we construct an equivalent Lagrangian using an auxiliary field  $\tilde{H}$  [1]:

$$\mathcal{L}_{AF} = (D_{\mu}\hat{H})^{\dagger}(D^{\mu}\hat{H}) + (D_{\mu}\hat{H})^{\dagger}(D^{\mu}\tilde{H}) + (D_{\mu}\tilde{H})^{\dagger}(D^{\mu}\hat{H}) + m_{\tilde{i}}^{2}\tilde{H}^{\dagger}\tilde{H} - V(\hat{H}). \tag{2.4}$$

One recovers the Lagrangian in Eq. (2.1) by substituting the equation of motion for the auxiliary field into Eq. (2.4) and integrating by parts. The kinetic terms are diagonalized by the field redefinition  $\hat{H} = H - \tilde{H}$ , yielding

$$\mathcal{L} = (D_{\mu}H)^{\dagger}(D^{\mu}H) - (D_{\mu}\tilde{H})^{\dagger}(D^{\mu}\tilde{H}) + m_{\tilde{h}}^{2}\tilde{H}^{\dagger}\tilde{H} - V(H - \tilde{H}). \tag{2.5}$$

The higher-derivative term has been eliminated at the expense of introducing the LW field  $\tilde{H}$  which has wrong-sign kinetic and mass terms.

The last two terms in Eq. (2.5) are extremized when the field H acquires a vacuum expectation value. In unitary gauge, one can write [1]

$$H = \begin{pmatrix} 0 \\ \frac{v+h}{\sqrt{2}} \end{pmatrix}, \quad \tilde{H} = \begin{pmatrix} \tilde{h}^+ \\ \frac{\tilde{h}+i\tilde{P}}{\sqrt{2}} \end{pmatrix}. \tag{2.6}$$

where  $v \approx 246$  GeV sets the electroweak scale. We will refer to h the ordinary Higgs field, and  $\tilde{h}$ ,  $\tilde{P}$ , and  $\tilde{h}^+$  as the LW scalar, pseudoscalar and charged Higgs fields, respectively. The Higgs field masses are determined by

$$\mathcal{L}_{\text{mass}} = -\frac{\lambda}{4} v^2 (h - \tilde{h})^2 + \frac{m_{\tilde{h}}^2}{2} (\tilde{h}\tilde{h} + \tilde{P}\tilde{P} + 2\tilde{h}^+\tilde{h}^-), \tag{2.7}$$

which shows mixing between the ordinary Higgs scalar and its LW partner. One can diagonalize the scalar mass matrix without altering the form the kinetic terms via a symplectic transformation:

$$\begin{pmatrix} h \\ \tilde{h} \end{pmatrix} = \begin{pmatrix} \cosh \theta & \sinh \theta \\ \sinh \theta & \cosh \theta \end{pmatrix} \begin{pmatrix} h_0 \\ \tilde{h}_0 \end{pmatrix}, \tag{2.8}$$

where subscript 0 indicates a mass eigenstate. The mixing angle  $\theta$  satisfies

$$\tanh 2\theta = \frac{-2m_h^2/m_{\tilde{h}}^2}{1 - 2m_h^2/m_{\tilde{h}}^2} = -\frac{2m_{h_0}^2 m_{\tilde{h}_0}^2}{m_{h_0}^4 + m_{\tilde{h}_0}^4},$$
(2.9)

with mass eigenvalues

$$m_{h_0}^2 = \frac{m_{\tilde{h}}^2}{2} \left( 1 - \sqrt{1 - \frac{4m_h^2}{m_{\tilde{h}}^2}} \right) \quad \text{and} \quad m_{\tilde{h}_0}^2 = \frac{m_{\tilde{h}}^2}{2} \left( 1 + \sqrt{1 - \frac{4m_h^2}{m_{\tilde{h}}^2}} \right).$$
 (2.10)

Notice that the eigenstate with "wrong-sign" kinetic terms is always the heavier of the two. The LW pseudoscalar  $\tilde{P}$  and LW charged scalar  $\tilde{h}^+$  have the same mass  $m_{\tilde{h}}$ . The masses of the neutral scalars are related to the mass of the pseudoscalar or charged Higgs by

$$m_{h_0}^2 + m_{\tilde{h}_0}^2 = m_{\tilde{h}}^2. (2.11)$$

As in the gauge sector, the LW partners to the SM fermions are decoupled from our effective theory. Even assuming realistic LW fermion masses of a few TeV, mixing between

ordinary and LW fermions is numerically small and can be ignored. The Yukawa couplings involving H and  $\tilde{H}$  are then given by [1]

$$\delta \mathcal{L} = \frac{\sqrt{2}}{v} \sum_{i} \left[ m_{u}^{i} \overline{u^{i}}_{R} (H - \tilde{H}) \epsilon Q_{L}^{i} - m_{d}^{i} \overline{d^{i}}_{R} (H^{\dagger} - \tilde{H}^{\dagger}) Q_{L}^{i} - m_{e}^{i} \overline{e^{i}}_{R} (H^{\dagger} - \tilde{H}^{\dagger}) L_{L}^{i} + \text{h.c.} \right],$$

$$(2.12)$$

where

$$Q_L = \begin{pmatrix} u_L \\ V d_L \end{pmatrix}, \qquad L_L = \begin{pmatrix} \nu \\ e_L \end{pmatrix}, \tag{2.13}$$

V is usual CKM matrix, and the fields are given in the mass eigenstate basis.

#### III. CONSTRAINING THE CHARGED HIGGS

The interaction between quarks and the charged Higgs field in LWSM can be extracted from Eq. (2.12),

$$\mathcal{L}_{\tilde{h}^{\pm}ff} = -\frac{g_2}{\sqrt{2}M_W}\tilde{h}^{+} \sum_{ij} \left[ m_u^i \bar{u}_R^i V_{ij} d_L^j + m_d^j \bar{u}_L^i V_{ij} d_R^j \right] + \text{ h.c.},$$
 (3.1)

while the  $\gamma$ -Higgs-Higgs and Z-Higgs-Higgs couplings follow from Eq. (2.5),

$$\mathcal{L}_{\tilde{h}^{+}\tilde{h}^{-}A,Z} = \left(ieA^{\mu} + i\frac{g_{2}\cos 2\theta_{W}}{2\cos\theta_{W}}Z^{\mu}\right)\left(\tilde{h}^{-}\partial_{\mu}\tilde{h}^{+} - \tilde{h}^{+}\partial_{\mu}\tilde{h}^{-}\right). \tag{3.2}$$

The analogous couplings in a Two-Higgs-Doublet Model (2HDM) of type II are given by [18]

$$\mathcal{L}_{h^{\pm}ff}^{2HDM} = \frac{g_2}{\sqrt{2}M_W} h^{+} \sum_{ij} \left[ \cot \beta m_u^i \bar{u}_R^i V_{ij} d_L^j + \tan \beta m_d^j \bar{u}_L^i V_{ij} d_R^j \right] + \text{ h.c.}$$
 (3.3)

and

$$\mathcal{L}_{h^+h^-A,Z}^{2HDM} = -\left(ieA^{\mu} + i\frac{g_2\cos 2\theta_W}{2\cos\theta_W}Z^{\mu}\right)\left(h^-\partial_{\mu}h^+ - h^+\partial_{\mu}h^-\right). \tag{3.4}$$

By comparing Eqs. (3.1) and (3.2) with Eqs. (3.3) and (3.4), we see that the charged Higgs interactions in the LWSM mimic those of the type-II 2HDM with  $\tan \beta = 1$ , except for overall signs. Hence, each occurrence of an  $\tilde{h}^+\tilde{h}^-\gamma$ ,  $\tilde{h}^+\tilde{h}^-Z$  or  $\tilde{h}^\pm \overline{q}q$  vertex in a Feynman diagram introduces a factor of -1 relative to the corresponding result in a type-II 2HDM. In addition, every charged Higgs propagator introduces another factor of -1, due to the wrong-sign LW quadratic terms. These observations allow us to modify the phenomenologically relevant, but sometimes complicated, next-to-leading order (NLO) calculations of loop amplitudes

in the type-II 2HDM to determine the numerical bounds on the LW Higgs sector. The processes that we consider below are ones that are enhanced by the large top quark Yukawa coupling; one would expect these to provide a reasonable picture of the allowed parameter space of the effective theory.

We consider  $B_q \bar{B}_q$  mixing for q = d or s, the inclusive decay  $B \to X_s \gamma$  and  $R_b \equiv \Gamma(Z \to b\bar{b})/\Gamma(Z \to \text{hadrons})$  to obtain bounds on the charged Higgs mass. These processes have been evaluated in the type-II 2HDM including NLO QCD corrections in Refs. [20], [21, 22, 23] and [24, 25], respectively. As described in the previous paragraph, we modify the 2HD model amplitudes to obtain bounds on the mass of the LW charged Higgs  $\tilde{h}^{\pm}$ .

## **A.** $B_q \overline{B}_q$ mixing

Before including the NLO QCD corrections, it is instructive to consider the leading-order (LO) result evaluated at the matching scale at which the exotic Higgs physics is integrated out. This scale is typically taken to be  $m_W$ . The mass splitting between  $B_q^0$  and  $\overline{B}_q^0$  mesons in the 2HDM of type II is then given by [19]

$$\Delta m_{B_{2HDM}} = \frac{G_F^2}{6\pi^2} m_W^2 |V_{tq} V_{tb}^*|^2 f_B^2 \hat{B}_{B_q} m_B \left( I_{WW} + \cot^2 \beta I_{Wh} + \cot^4 \beta I_{hh} \right) . \tag{3.5}$$

Here  $I_{WW}$  originates from the pure  $W^{\pm}$ -exchange Feynman diagrams shown in Fig. 1,  $I_{Wh}$  from the single-charged-Higgs-exchange diagrams in Fig. 2, and  $I_{hh}$  from the pure charged-Higgs-exchange diagrams shown in Fig. 3. These functions are given by [19]

$$I_{WW} = \frac{x}{4} \left( 1 + \frac{9}{(1-x)} - \frac{6}{(1-x)^2} - \frac{6}{x} \left( \frac{x}{1-x} \right)^3 \ln x \right),$$

$$I_{Wh} = \frac{xy}{4} \left[ -\frac{8-2x}{(1-x)(1-y)} + \frac{6z \ln x}{(1-x)^2(1-z)} + \frac{(2z-8) \ln y}{(1-y)^2(1-z)} \right],$$

$$I_{hh} = \frac{xy}{4} \left[ \frac{(1+y)}{(1-y)^2} + \frac{2y \ln y}{(1-y)^3} \right],$$
(3.6)

where  $x = m_t^2/m_W^2$ ,  $y = m_t^2/m_{\tilde{h}}^2$  and  $z = x/y = m_{\tilde{h}}^2/m_W^2$ .

To obtain the mass splitting appropriate to the LWSM, we set  $\tan \beta = 1$ . We must multiply  $I_{Wh}$  by  $(-1)^3 = -1$ , which takes into account two  $f\bar{f}\tilde{h}^{\pm}$  vertices and one  $\tilde{h}^{\pm}$  propagator; we multiply  $I_{hh}$  by  $(-1)^6 = 1$  because there are four  $f\bar{f}\tilde{h}^{\pm}$  vertices and two  $\tilde{h}^{\pm}$  propagators. Therefore, for the LWSM, one finds the LO result

$$\Delta m_{B_{LWSM}} = \frac{G_F^2}{6\pi^2} m_W^2 \left| V_{tq} V_{tb}^* \right|^2 f_B^2 \hat{B}_{B_q} m_B \left( I_{WW} - I_{Wh} + I_{hh} \right)$$
 (3.7)



FIG. 1: SM diagrams for  $B\bar{B}$  mixing. Wavy lines represent W bosons and solid lines represent quarks.

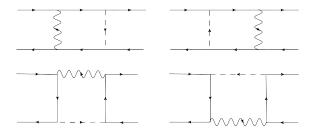


FIG. 2: New physics diagrams for  $B\bar{B}$  mixing with one W and one charged Higgs exchanged. Dashed lines represent charged Higgs fields, wavy lines represent W bosons and solid lines represent quarks. These diagrams are proportional with  $\cot^2 \beta$  in the type-II 2HDM and flip overall sign in the LWSM.

Our numerical values for the particle masses, CKM elements  $V_{ij}$ ,  $G_F$ , the decay constant  $f_B$  and the bag factor  $\hat{B}_{Bq}$  are given in Appendix A. Using these, we plot the LO  $B_d - \bar{B}_d$  mass splitting in the LWSM and in a type-II 2HDM with  $\tan \beta = 1$  in Fig. 4. The new physics diagrams in the 2HDM give a positive contribution to the mass splitting. In the LWSM, however, the mass splitting receives a negative contribution since the  $I_{Wh}$  term flips sign and dominates over  $I_{hh}$ . Since the magnitude of  $I_{Wh}$  is comparable to that of  $I_{WW}$ , the new physics can significantly alter the Standard Model prediction, leading to useful bounds on the mass of the charged Higgs when the result is compared to the experimental value.

To do such a comparison, however, we work with the NLO result that includes QCD



FIG. 3: New physics diagrams for  $B\bar{B}$  mixing with two charged Higgs particles exchanged. Dashed lines represent charged Higgs fields and solid lines represent quarks. These diagrams are proportional with  $\cot^4 \beta$  in 2HDM and and have the same sign in the LWSM.

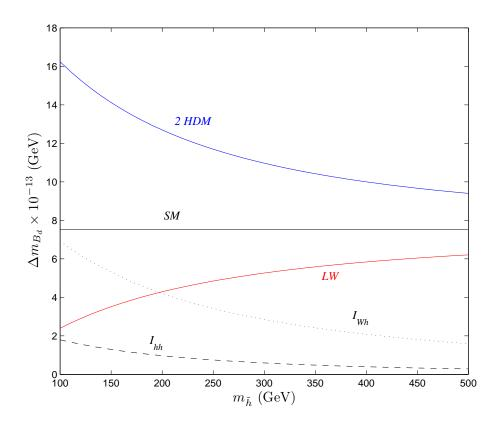


FIG. 4: The mass splitting  $\Delta m_{B_d}$  predicted at LO in the LWSM and in type-II 2HDM with  $\tan \beta = 1$ , as functions of the charged Higgs mass. The solid lines represents the predictions of the 2HDM, the Standard Model and LWSM, as labelled. The dashed line gives  $\frac{G_F^2}{6\pi^2}m_W^2\left(V_{tq}V_{tb}^*\right)^2 f_B^2\hat{B}_{B_d}m_{B_d} \times I_{Wh}$  and dotted line gives  $\frac{G_F^2}{6\pi^2}m_W^2\left(V_{tq}V_{tb}^*\right)^2 f_B^2\hat{B}_{B_d}m_{B_d} \times I_{hh}$ .

corrections and takes into account running between the matching scale  $m_W$  and the scale of the B-mesons. Unlike Eq. (3.6), these amplitudes are quite complicated and cannot be summarized in a few lines. However, the approach for modifying them to obtain LWSM results is precisely the same as in our simple leading order example. We use the NLO amplitudes given in Ref. [20] for our numerical analysis. Our predictions depend on the bag factor which is the largest source of theoretical uncertainty. We use lattice QCD estimates of the bag factors given in Ref. [27]:  $f_B\sqrt{\hat{B}_{B_d}}=216\pm15$  GeV and  $f_B\sqrt{\hat{B}_{B_s}}=266\pm18$  GeV. For other inputs, we use the values given in Appendix A.

There is an immediate question on the proper choice for the CKM matrix elements required to produce a theoretical prediction. These elements are extracted, in part, from global fits that include the very process that is affected by the new physics. The simplest approach (and one that seems standard in the literature) is to use the best global fit values for the CKM elements in the SM. One then requires that the theoretical prediction for the process of interest not deviate by more than a prescribed amount (approximately two standard deviations) from the experimental value. This approach is sensible because the global SM fit of CKM elements is consistent with the experimental data. More precisely, our bounds are determined using a  $\chi^2$  test:

$$\chi_i^2 = \frac{(\mathcal{O}_{i,LWSM} - \mathcal{O}_{i,expt})^2}{\sigma_i^2},\tag{3.8}$$

where  $\mathcal{O}_{i,LWSM}$  is LWSM prediction for a particular process,  $\mathcal{O}_{i,expt}$  is the related experimental result and  $\sigma_i$  incorporates the error coming from both the theoretical prediction and the experimental result. We require that  $\chi_i^2$  can not exceed 3.84 in order to determine the 95% C.L. bound on the charged Higgs mass. Theoretical uncertainties (described above) are added in quadrature with the experimental error in applying the  $\chi^2$  test. We assume the experimental values [26]  $\Delta m_{B_d} = (3.337 \pm 0.033) \times 10^{-10}$  MeV and  $\Delta m_{B_s} = (117.0 \pm 0.8) \times 10^{-10}$  MeV. The results of this analysis are shown in Figs. 5 and 6. With the main theoretical error originating from the bag factors, we find that the total

With the main theoretical error originating from the bag factors, we find that the total error in both the  $B_d$  and  $B_s$  systems is well approximated by

$$\sigma = 0.14 \times \Delta m_{B_{LWSM}},\tag{3.9}$$

which reflects that the experimental uncertainty is negligible compared to the theoretical one. Applying our  $\chi^2$  test to  $B_d\bar{B}_d$  mixing, we find that the mass of LW charged Higgs boson is bounded by

$$m_{\tilde{h}} > 303 \text{ GeV} \qquad (95\% \text{ C.L.}),$$
 (3.10)

while from  $B_s\bar{B}_s$  mixing,

$$m_{\tilde{h}} > 354 \text{ GeV}$$
 (95% C.L.). (3.11)

Note that the bound from  $B_d\bar{B}_d$  is almost identical in the type-II 2HDM with  $\tan\beta = 1$ , where one would find  $m_{h^\pm} > 308$  GeV using the same method of analysis. However, this is purely coincidental. If the theoretical uncertainties were reduced by a factor of 2 one would find that these particular bounds change to 446 GeV (LWSM) and 618 GeV (2HDM,  $\tan\beta = 1$ ), consistent with our earlier comment that the predictions in these two theories are qualitatively different.

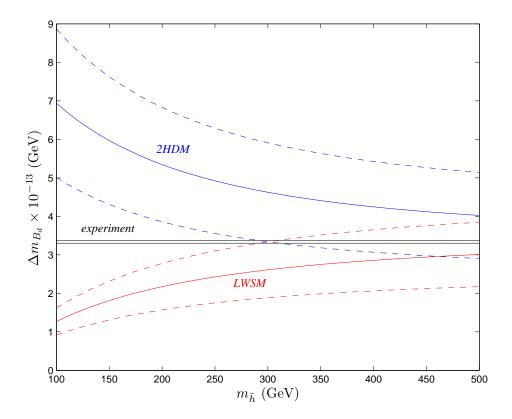


FIG. 5:  $B_d - \bar{B}_d$  mass splitting predictions in the 2HDM of type-II with  $\tan \beta = 1$  and in the LWSM, as functions of the charged Higgs mass. The solid curved lines give the central values of the theoretical predictions, while the dashed lines delimit their  $2\sigma$  error bands. The solid horizontal lines give the  $2\sigma$  experimentally allowed region.

**B.** 
$$B \to X_s \gamma$$

The bounds presented in Eqs. (3.10) and (3.11) were limited by the theoretical uncertainties in the lattice calculations of the bag factors. We now consider an observable that does not have this uncertainty, namely the ratio of the inclusive B decay width  $\Gamma(B \to X_s \gamma)$  to  $\Gamma(B \to X_c e \overline{\nu}_e)$ . Standard model diagrams for  $B \to X_s \gamma$  are shown in Fig. 7 and new physics diagrams in Fig. 8. In the LWSM, the diagrams of Fig. 8 differ by an overall sign relative to those of a type-II 2HDM with  $\tan \beta = 1$ .

As in our discussion of  $B\bar{B}$  mixing, we first consider the leading-order contributions to  $B \to X_s \gamma$ , evaluated at the matching scale  $m_W$ , to gain some insight on the effect of new

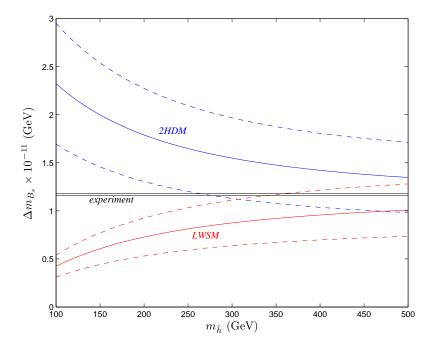


FIG. 6:  $B_s - \bar{B}_s$  mass splitting predictions in the 2HDM of type-II with  $\tan \beta = 1$  and in the LWSM, as functions of the charged Higgs mass. The solid curved lines give the central values of the theoretical predictions, while the dashed lines delimit their  $2\sigma$  error bands. The solid horizontal lines give the  $2\sigma$  experimentally allowed region.

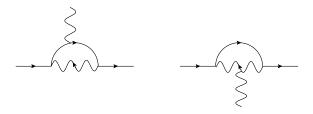


FIG. 7: SM contributions to  $B \to X_s \gamma$ . Wavy lines with (without) arrows represent W bosons (photons), and solid lines represent quarks.



FIG. 8: Charged Higgs contributions to  $B \to X_s \gamma$ . Dashed lines represent Higgs fields, solid lines represent quarks and wavy lines represent photons.

physics. The branching fraction is given by [28]

$$\mathcal{B}(B \to X_s \gamma) = \mathcal{B}(B \to X_c e \bar{\nu}_e) \left| \frac{V_{ts}^* V_{tb}}{V_{cb}} \right|^2 \frac{6\alpha_{em}}{\pi f(m_c^2/m_b^2)} \left| C_{7,SM}^0 + C_{7,NP}^0 \right|^2, \tag{3.12}$$

where  $C_7^0$  are Wilson coefficients. In the 2HDM of type II, these are given by [28]

$$C_{7,SM}^{0} = \frac{x}{24} \left[ \frac{-8x^3 + 3x^2 + 12x - 7 + (18x^2 - 12x)\ln(x)}{(x-1)^4} \right], \tag{3.13}$$

$$C_{7,NP}^{0} = \frac{1}{3}\cot^{2}(\beta) C_{7,SM}^{0}(x \to y) + \frac{1}{12}y \left[ \frac{-5y^{2} + y - 3 + (6y - 4)\ln(y)}{(y - 1)^{3}} \right], \qquad (3.14)$$

where  $x = \frac{m_t^2}{m_W^2}$  and  $y = \frac{m_t^2}{m_H^2}$ , while in the LWSM

$$C_{7,NP}^{0} = -\frac{1}{3}C_{7,SM}^{0}(x \to y) - \frac{1}{12}y \left[ \frac{-5y^2 + y - 3 + (6y - 4)\ln(y)}{(y - 1)^3} \right]. \tag{3.15}$$

The function f is a phase space suppression factor from the semileptonic decay rate

$$f(z) = 1 - 8z_0 + 8z_0^3 - z_0^4 - 12z_0^2 \ln z_0, (3.16)$$

where  $z_0 = m_c^2/m_b^2$ . A plot of Wilson coefficients  $C_7^0$  is provided in Fig. 9. This figure indicates that the new physics gives a positive contribution to branching fraction in the 2HDM, but a negative one in the LWSM, leading to a difference in the bound on the mass of the charged Higgs.

Following the approach used in the previous subsection, we obtain more accurate numerical bounds by modifying the 2HDM results that include NLO QCD corrections. These expressions cannot be summarized in a few lines, and are taken from Ref. [21]. All relevant input parameters are given in Appendix A. As discussed in Ref. [21], the theoretical uncertainty comes from the error bars on physical input parameters as well as the choice of a number of renormalization scales. The scales  $\mu_b$  and  $\bar{\mu}_b$  defined in Ref. [21] refer to the B meson renormalization scale in the  $b \to X_s \gamma$  and  $b \to X_c e \bar{\nu}_e$  amplitudes, respectively, while  $\mu_W$  is the scale at which the full theory is matched to the low-energy effective theory. The theoretical error is determined, in part, by varying these scales from half to twice of their central values. Errors coming from varying these scales and those originating from input parameters uncertainties are added in quadrature to obtain a total theoretical error. The experimentally allowed range is given by  $\mathcal{B}(B \to X_s \gamma) = (3.52 \pm 0.23 \pm 0.09) \times 10^{-4}$  [29]. Our results for the LWSM and for the type-II 2HDM with  $\tan \beta = 1$  are plotted in Fig. 10.

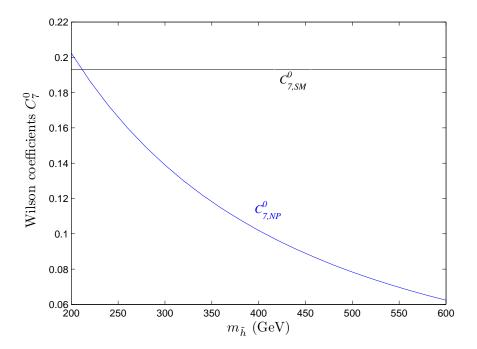


FIG. 9: Contributions to the Wilson coefficient  $C_7^0$  from the Standard Model (SM) and from New Physics (NP). The curve labelled  $C_{7,NP}^0$  corresponds to the 2HDM with  $\tan \beta = 1$  or  $-C_{7,NP}^0$  for the LWSM.

Note that the theoretical predictions asymptote at large values of the charged Higgs mass to the Standard Model prediction  $\mathcal{B}(B \to X_s \gamma) = (3.60 \pm 0.36) \times 10^{-4}$ .

The bound on the charged Higgs mass is obtained by using the  $\chi^2$  test described in the previous subsection. Including the NLO QCD corrections, the bound in the LWSM is

$$m_{\tilde{h}} > 463 \text{ GeV}$$
 (95% C.L.). (3.17)

In Fig. 10 we display  $1\sigma$  theoretical and experimental error bands. Note that for approximately equal errors  $\sigma_0$ , the separation between the experimental and theoretical central values that corresponds to a  $\chi^2$  of 3.84 is  $\sim 2.8 \sigma_0$ . Using this observation, one can confirm that the bound in Eq. (3.17) and Fig. 10 are consistent.

### C. $R_b$ from Z Decay

The bounds that we have obtained thus far have followed from the consideration of flavor changing neutral current processes. It is also interesting to consider the effect of new Higgs

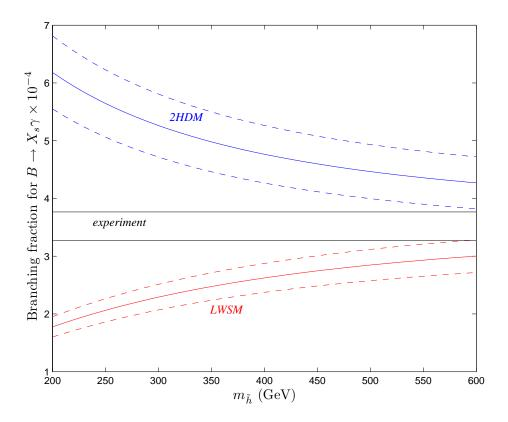


FIG. 10: Predictions for the branching fraction  $\mathcal{B}(B \to X_s \gamma)$  in the type-II 2HDM with  $\tan \beta = 1$  and in the LWSM as functions of the charged Higgs mass. The solid curved lines give the central values of the theoretical predictions, while the dashed lines delimit their  $1\sigma$  error bands. The solid horizontal lines give the  $1\sigma$  experimentally allowed region.

physics on the flavor-conserving  $Zb\bar{b}$  coupling, which is measured to high precision. Here we focus on the observable  $R_b \equiv \Gamma(Z \to b\bar{b})/\Gamma(Z \to \text{hadrons})$ . The charged-Higgs diagrams that contribute to this process are shown in Fig. 11, while the neutral Higgs diagrams are shown in Fig. 12. We will argue that the top-Yukawa-enhanced charged Higgs diagrams are the only one necessary to obtain a numerically accurate result, and that the LWSM prediction can be obtained, as before, by modifying the 2HD model result, which can be found, in this case, in Ref. [25].

Let us first consider the possible contribution from the neutral Higgs fields. The interaction Lagrangian involving the neutral Higgs fields and quarks is given by

$$\mathcal{L}_{Hff} = -\sum_{f} \frac{m_f}{v} \left\{ (\cosh \theta - \sinh \theta) h_0 + (\sinh \theta - \cosh \theta) \tilde{h}_0 + i \tilde{P} \right\} \bar{f}_R f_L + \text{ h.c.}, \quad (3.18)$$

where sum extends over all fermions in the SM. The interactions between the Z-boson and the neutral Higgs fields are given by:

$$\mathcal{L}_{ZHH} = \frac{g_2}{2\cos\theta_W} \left[ \sinh\theta \left( h_0 \partial\mu \tilde{P} - \tilde{P}\partial_\mu h_0 \right) + \cosh\theta \left( \tilde{h}_0 \partial\mu \tilde{P} - \tilde{P}\partial_\mu \tilde{h}_0 \right) \right] Z^\mu, \tag{3.19}$$

and

$$\mathcal{L}_{ZZH} = \frac{g_2 m_Z}{2 \cos \theta_W} Z_\mu^2 \left( \cosh \theta h_0 + \sinh \theta \tilde{h}_0 \right). \tag{3.20}$$

Clearly the neutral Higgs amplitudes that contribute to  $R_b$  are smaller than those of the charged Higgs by  $m_b^2/m_t^2 \sim 6 \times 10^{-4}$  and can be neglected provided that there is no compensating enhancement from any other source. One might worry in the LWSM that the factors of  $\cosh\theta$  and  $\sinh\theta$ , which can be arbitrarily large, might provide such an effect. This fear, however, is unfounded. Every relevant  $Z \to b\bar{b}$  amplitude could have been computed in the HD formulation of the LWSM where there are clearly no couplings that are becoming large. The particle mass eigenvalues and the hyperbolic functions of mixing angles in the LW form of the theory must therefore combine in physical amplitudes so that the same outcome is obtained. As a pedagogical example, one can consider the diagrams with fermion wave function renormalization due to a Higgs field loop shown in Fig. 12. The product of the scalar propagators and fermion couplings is proportional to

$$(\cosh \theta - \sinh \theta)^2 \left[ \frac{i}{p^2 - m_{h_0}^2} - \frac{i}{p^2 - m_{\tilde{h}_0}^2} \right],$$
 (3.21)

where p is the internal momentum on the scalar line. From Eq. (2.10) it follows that

$$\begin{split} m_{h_0}^2 + m_{\tilde{h}_0}^2 &= m_{\tilde{h}}^2 \,, \\ m_{h_0}^2 \, m_{\tilde{h}_0}^2 &= m_h^2 \, m_{\tilde{h}}^2 \\ m_{h_0}^2 - m_{\tilde{h}_0}^2 &= -m_h^2 \sqrt{1 - 4m_h^2/m_{\tilde{h}}^2} \,, \end{split} \tag{3.22}$$

and using Eq. (2.9)

$$(\cosh \theta - \sinh \theta)^2 = \frac{1}{\sqrt{1 - 4m_h^2/m_{\tilde{h}}^2}}$$
 (3.23)

from which one can easily show that Eq. (3.21) can be rewritten

$$\frac{i}{p^2 - m_h^2 - p^4/m_{\tilde{h}}^2},\tag{3.24}$$

which has no singular behavior as either hyperbolic function becomes infinite. It is therefore safe to drop  $m_b^2/m_t^2$  suppressed effects, as is usually done in conventional 2HD models.

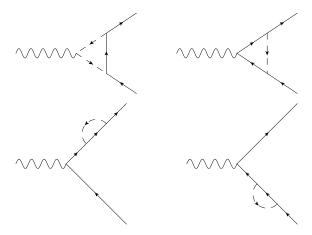


FIG. 11: Charged Higgs contributions to  $Z \to b\bar{b}$  decay. Wavy lines represent Z bosons, solid lines represent quarks and dashed lines represent charged Higgs fields.

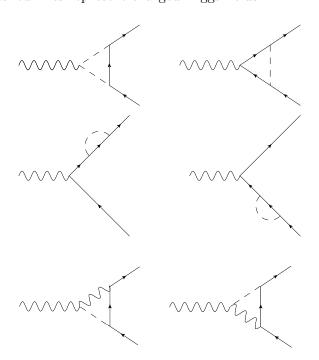


FIG. 12: Neutral Higgs contributions to  $Z \to b\bar{b}$  decay. Wavy lines represent Z bosons, solid lines represent quarks and dashed lines represent neutral Higgs fields (scalars and pseudoscalar).

In the type-II 2HDM, the corrections to the left- and right-handed b-quark couplings to the Z boson are given by [25]

$$\delta g^{L} = \frac{1}{32\pi^{2}} \left( \frac{g_{2}m_{t}}{\sqrt{2}m_{W}} \cot \beta \right)^{2} \frac{e}{s_{W}c_{W}} \left[ \frac{R}{R-1} - \frac{R \ln R}{(R-1)^{2}} \right],$$

$$\delta g^{R} = -\frac{1}{32\pi^{2}} \left( \frac{g_{2}m_{b}}{\sqrt{2}m_{W}} \tan \beta \right)^{2} \frac{e}{s_{W}c_{W}} \left[ \frac{R}{R-1} - \frac{R \ln R}{(R-1)^{2}} \right],$$
(3.25)

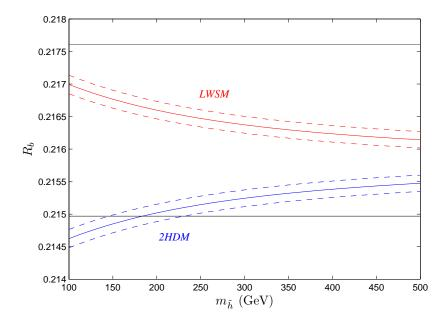


FIG. 13:  $R_b$  predictions for the 2HDM of type-II with  $\tan \beta = 1$  and for the LWSM as functions of the charged Higgs mass. The solid curved lines give the central values of the theoretical predictions, while the dashed lines delimit their  $2\sigma$  error bands. The solid horizontal lines give the  $2\sigma$  experimentally allowed region.

where  $R = m_t^2/m_{\tilde{h}}^2$ . For  $\tan \beta \simeq 1$ , the correction  $\delta g^R$  is negligible since it is  $O(m_b^2/m_t^2)$  smaller than  $\delta g^L$ . Therefore, the leading correction to the  $Zb\bar{b}$  vertex in the LWSM is given by

$$\delta g^{L} = -\frac{1}{32\pi^{2}} \left(\frac{g_{2}m_{t}}{\sqrt{2}m_{W}}\right)^{2} \frac{e}{s_{W}c_{W}} \left[\frac{R}{R-1} - \frac{R\ln R}{(R-1)^{2}}\right]. \tag{3.26}$$

In the Standard Model, the best global fit value for  $R_b$  is  $0.21629 \pm 0.00066$ , while the Standard Model prediction is  $0.21584\pm0.00006$  [26]; the LWSM gives a positive contribution to  $R_b$  which helps reconcile the central values. The results in a type-II 2HDM with  $\tan \beta = 1$  and in the LWSM are plotted in Fig. 13. Since the LWSM correction pushes  $R_b$  toward its experimental value, we do not obtain any bound on the charged Higgs mass from this process.

### IV. CONSTRAINING THE NEUTRAL SECTOR

It is worth recalling that the parameter we have been bounding,  $m_{\tilde{h}}$ , determines both the charged and pseudoscalar LW Higgs masses. Bounds as high as those obtained in the previous section easily supercede those of direct collider searches for charged Higgs bosons in type-II 2HD models, which are typically below 80 GeV [26]. These bounds should apply to the LWSM since the overall sign-flips in the tree-level diagrams that determine the direct production of charged LW Higgs do not affect the production rate.

We now consider what can be said about the allowed parameter space for the remaining, scalar LW Higgs fields. We determine the allowed region in the  $m_{h_0}$ - $m_{\tilde{h}_0}$  mass eigenvalue plane, the most convenient parameter space for comparison to future collider searches. From Eq. (2.11), which relates the masses of the charged and neutral scalars, and using our strongest bound on  $m_{\tilde{h}}$  from  $B \to X_s \gamma$ , we have

$$m_{h_0}^2 + m_{\tilde{h}_0}^2 > (463 \text{ GeV})^2$$
. (4.1)

As noted earlier, Eq. (2.10) implies that

$$m_{\tilde{h}_0} > m_{h_0} \,.$$
 (4.2)

Together, Eqs. (4.1) and (4.2) lead to a lower bound on the  $\tilde{h}_0$  mass

$$m_{\tilde{h}_0} > 327 \text{ GeV}.$$
 (4.3)

Finally, searches for the Higgs at LEP allows us to determine a direct bound on  $m_{h_0}$ . At LEP, the Higgs is produced via the Higgstrahlung process  $e^+e^- \to Z^* \to h_0 Z$ , which involves the vertex given in Eq. (3.20). Taking into account the bound on  $m_{\tilde{h}_0}$  in Eq. (4.3), and the kinematical range accessible at LEP we conclude that the  $h_0$  and  $\tilde{h}_0$  are well separated and we can neglect effects due to the  $\tilde{h}_0$  which may contribute to the same final states (e.g.,  $e^+e^- \to Zb\bar{b}$ ). The  $h_0ZZ$  coupling differs from the Standard Model by a factor of  $\cosh\theta$ , but this exceeds the Standard Model value  $\cosh\theta = 1$  by no more than 1% in the LEP search. In addition, a factor of  $(\cosh\theta - \sinh\theta)$  that appears in the Higgs couplings to fermions [c.f. Eq. (3.18)] does so universally, and even enhances the branching fraction to these modes compared to the far subleading three-body decay channels. Thus, referring to Ref. [30], we expect the LEP lower bound

$$m_{h_0} > 114 \text{ GeV}.$$
 (4.4)

to be approximately valid, and at the very least, to be slightly below the actual bound that could have been obtained if LEP did a dedicated Lee-Wick analysis.

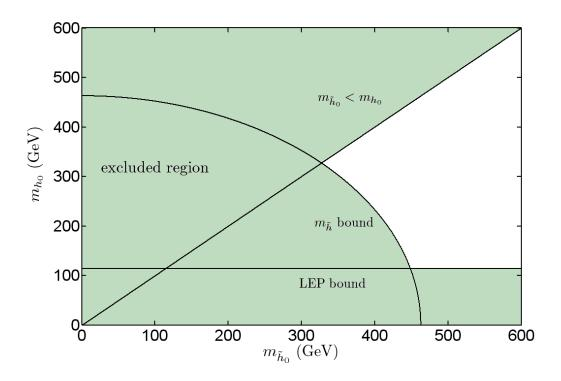


FIG. 14: Bounds on the  $m_{h_0}$ - $m_{\tilde{h}_0}$  plane. The shaded region is excluded

We plot the excluded regions in the  $m_{h_0}$ - $m_{\tilde{h}_0}$  plane in Fig. 14. The shaded quarter circle represents the indirect constraint obtained from our charged Higgs bound Eq. (4.1), the horizontal line represents the LEP bound Eq. (4.4), and the diagonal line indicates where Eq. (4.2) holds.

### V. CONCLUSIONS

We have studied the possibility that the Higgs sector of the Lee-Wick Standard Model is lighter than the remaining Lee-Wick particle content, a possibility that is consistent with Higgs sector naturalness and precision electroweak constraints. The effective theory is a two-Higgs doublet model in which one doublet has wrong-sign kinetic and mass terms. By considering  $B_d$ - $\overline{B}_d$  and  $B_s$ - $\overline{B}_s$  mixing and the decay  $b \to X_s \gamma$ , we obtained the bounds  $m_{\tilde{h}} > 303$  GeV, 354 GeV and 463 GeV, respectively, where  $m_{\tilde{h}}$  is the mass of the Lee-Wick charged Higgs  $\tilde{h}^{\pm}$  and also the mass of the Lee-Wick pseudoscalar  $\tilde{P}$ . We then studied the decay  $Z \to b\bar{b}$  and found that the Lee-Wick Higgs corrections to the Stardard Model prediction provided better agreement with the experimental data and that no additional

bound could be obtained. Finally, we argued the LEP search for the Higgs boson implies the bound  $m_{h_0} > 114$  GeV on the ordinary Higgs scalar in the Lee-Wick Standard Model. Study of the allowed regions of the  $m_{h_0}$ - $m_{\tilde{h}_0}$  plane led us to an absolute lower bound on the Lee-Wick neutral scalar mass  $m_{\tilde{h}_0} > 327$  GeV. Interestingly, all our bounds indicate that the Lee-Wick Higgs sector could be within the kinematic reach of the LHC.

Clearly, a vast literature exists on two-Higgs doublet model constraints and collider signals — other processes surely exist to which the present analysis could be extended. The work reported here is intended as a first step in exploring a two-Higgs doublet model of an unconventional sort, and a reminder that Lee-Wick physics can conceivably lurk well below 1 TeV.

### Acknowledgments

We thank the NSF for support under Grant Nos. PHY-0456525 and PHY-0757481.

### APPENDIX A: NUMERICAL INPUTS

Unless referenced otherwise below, the numerical inputs used in our analysis are taken from Particle Data Group [26]:

Quarks, gauge bosons and B mesons masses		
$m_t = 171.2 \pm 2.1 \text{ GeV}$	$m_W = 80.398 \pm 0.025 \text{ GeV}$	
$\bar{m}_b(\bar{m}_b) = 4.2^{+0.17}_{-0.07} \text{ GeV}$	$m_Z = 91.1876 \pm 0.0021 \text{ GeV}$	
$\bar{m}_c(\bar{m}_c) = 1.27^{+0.07}_{-0.11} \text{ GeV}$	$m_{B_d} = 5279.53 \pm 0.33 \text{ MeV}$	
$m_s = 104^{+26}_{-34} \text{ MeV}$	$m_{B_s} = 5366.3 \pm 0.6 \text{ MeV}$	

Wolfenstein parameters	
$\lambda = 0.2257^{+0.0009}_{-0.0010}$	$A = 0.814^{+0.021}_{-0.022}$
$\bar{\rho} = 0.135^{+0.031}_{-0.016}$	$\bar{\eta} = 0.349^{+0.015}_{-0.017}$

(The relationship between the Wolfenstein parameters and the  $V_{ij}$  that preserves unitarity to all orders in  $\lambda$  can be found in Ref. [26].)

Other parameters	
$G_F = 1.16637 \times 10^{-5} \text{ GeV}^{-2}$	$\alpha_{em}^{-1} = 137.035999679$
$\alpha_s(m_Z) = 0.1176 \pm 0.0020$	$s_W^2 = 0.23119 \pm 0.00014$
$f_B \sqrt{\hat{B}_{B_d}} = 216 \pm 15 \text{ GeV } [27]$	$\mathcal{B}(B \to X_c e \bar{\nu}_e) = (10.74 \pm 0.16)\% [29]$
$f_B \sqrt{\hat{B}_{B_s}} = 266 \pm 18 \text{ GeV } [27]$	$(m_B^2 - m_{B^*}^2)/4 = 0.12 \text{ GeV}^2$

Note that the top quark mass is the pole mass, while the remaining quark masses are running masses in the  $\overline{MS}$  scheme.

B. Grinstein, D. O'Connell and M. B. Wise, Phys. Rev. D 77, 025012 (2008) [arXiv:0704.1845 [hep-ph]].

- [5] S. Coleman, in Subnuclear Phenomena, edited by A. Zichichi (Academic, New York, 1970), p. 282.
- [6] B. Grinstein, D. O'Connell and M. B. Wise, arXiv:0805.2156 [hep-th].
- [7] B. Grinstein, D. O'Connell and M. B. Wise, Phys. Rev. D 77, 065010 (2008) [arXiv:0710.5528 [hep-ph]].
- [8] K. Jansen, J. Kuti and C. Liu, Phys. Lett. B 309, 119 (1993) [arXiv:hep-lat/9305003]; Phys. Lett. B 309, 127 (1993) [arXiv:hep-lat/9305004]; C. Liu, arXiv:0704.3999 [hep-ph]; A. van Tonder, Int. J. Mod. Phys. A 22, 2563 (2007) [arXiv:hep-th/0610185]; arXiv:0810.1928 [hep-th]; Z. Fodor, K. Holland, J. Kuti, D. Nogradi and C. Schroeder, PoS LAT2007, 056 (2007) [arXiv:0710.3151 [hep-lat]]; F. Knechtli, N. Irges and M. Luz, arXiv:0711.2931 [hep-ph].
- [9] T. G. Rizzo, JHEP 0706, 070 (2007) [arXiv:0704.3458 [hep-ph]]; 0801, 042 (2008) [arXiv:0712.1791 [hep-ph]].
- [10] T. R. Dulaney and M. B. Wise, Phys. Lett. B 658, 230 (2008) [arXiv:0708.0567 [hep-ph]];
- [11] E. Alvarez, L. Da Rold, C. Schat and A. Szynkman, JHEP 0804, 026 (2008) [arXiv:0802.1061 [hep-ph]]; arXiv:0810.3463 [hep-ph]; T. E. J. Underwood and R. Zwicky, Phys. Rev. D 79,

<sup>[2]</sup> T. D. Lee and G. C. Wick, Nucl. Phys. B 9, 209 (1969).

<sup>[3]</sup> T. D. Lee and G. C. Wick, Phys. Rev. D 2, 1033 (1970).

<sup>[4]</sup> R. E. Cutkosky, P. V. Landshoff, D. I. Olive and J. C. Polkinghorne, Nucl. Phys. B 12, 281 (1969).

- 035016 (2009) [arXiv:0805.3296 [hep-ph]].
- [12] C. D. Carone and R. F. Lebed, Phys. Lett. B 668, 221 (2008) [arXiv:0806.4555 [hep-ph]].
- [13] C. D. Carone and R. F. Lebed, JHEP **0901**, 043 (2009) [arXiv:0811.4150 [hep-ph]].
- [14] B. Grinstein and D. O'Connell, Phys. Rev. D 78, 105005 (2008) [arXiv:0801.4034 [hep-ph]].
- [15] C. D. Carone, Phys. Lett. B 677, 306 (2009) [arXiv:0904.2359 [hep-ph]].
- [16] B. Fornal, B. Grinstein and M. B. Wise, Phys. Lett. B 674, 330 (2009) [arXiv:0902.1585 [hep-th]].
- [17] A. Rodigast and T. Schuster, Phys. Rev. D 79, 125017 (2009) [arXiv:0903.3851 [hep-ph]];
  A. M. Shalaby, arXiv:0812.3419 [hep-th]; S. Lee, arXiv:0810.1145 [astro-ph]; F. Wu and M. Zhong, Phys. Rev. D 78, 085010 (2008) [arXiv:0807.0132 [hep-ph]]; J. R. Espinosa, B. Grinstein, D. O'Connell and M. B. Wise, Phys. Rev. D 77, 085002 (2008) [arXiv:0705.1188 [hep-ph]]; F. Krauss, T. E. J. Underwood and R. Zwicky, Phys. Rev. D 77, 015012 (2008) [arXiv:0709.4054 [hep-ph]];
- [18] J. F. Gunion and H. E. Haber, Nucl. Phys. B **272**, 1 (1986) [Erratum-ibid. B **402**, 567 (1993)].
- [19] J. F. Gunion, H. E. Haber, G. L. Kane and S. Dawson, "The Higgs Hunter's Guide," Cambridge, MA: Perseus (1990) 425 p.
- [20] J. Urban, F. Krauss, U. Jentschura and G. Soff, Nucl. Phys. B 523, 40 (1998) [arXiv:hep-ph/9710245].
- [21] M. Ciuchini, G. Degrassi, P. Gambino and G. F. Giudice, Nucl. Phys. B **527**, 21 (1998) [arXiv:hep-ph/9710335].
- [22] F. Borzumati and C. Greub, Phys. Rev. D 58, 074004 (1998) [arXiv:hep-ph/9802391].
- [23] P. Gambino and M. Misiak, Nucl. Phys. B **611**, 338 (2001) [arXiv:hep-ph/0104034].
- [24] A. Denner, R. J. Guth, W. Hollik and J. H. Kuhn, Z. Phys. C 51, 695 (1991).
- [25] H. E. Haber and H. E. Logan, Phys. Rev. D **62**, 015011 (2000) [arXiv:hep-ph/9909335].
- [26] C. Amsler *et al.* [Particle Data Group], Phys. Lett. B **667**, 1 (2008).
- [27] E. Gamiz, C. T. H. Davies, G. P. Lepage, J. Shigemitsu and M. Wingate [HPQCD Collaboration], arXiv:0902.1815 [hep-lat].
- [28] B. Grinstein and M. B. Wise, Phys. Lett. B **201**, 274 (1988).
- [29] E. Barberio et al. [Heavy Flavor Averaging Group], arXiv:0808.1297 [hep-ex].
- [30] R. Barate *et al.* [LEP Working Group for Higgs boson searches and ALEPH Collaboration and DELPHI Collaboration and L3 Collaboration and OPAL Collaboration ], Phys. Lett. B

 ${\bf 565},\, 61 \,\, (2003) \,\, [{\rm arXiv:hep\text{-}ex}/0306033].$